Inorg. Chem. **2006**, *45*, 8551–8562

Isomeric Distribution and Catalyzed Isomerization of Cobalt(III) Complexes with Pentadentate Macrocyclic Ligands. Importance of Hydrogen Bonding

Gabriel Aullón,[†] Paul V. Bernhardt,[‡] Fernando Bozoglián,[†] Mercè Font-Bardía,[§] Brendan P. Macpherson,[‡] Manuel Martínez,*[,†] Carlos Rodríguez,[†] and Xavier Solans[§]

Departament de Química Inorgànica, Universitat de Barcelona, Martí i Franquès 1-11, E-08028 Barcelona, Spain, Department of Chemistry, University of Queensland, Brisbane 4072, Australia, and Departament de Mineralogia, Cristal·lografia i Dipòsits Minerals, Universitat de Barcelona, Martí i Franquès s/n, E-08028 Barcelona, Spain

Received April 28, 2006

We have investigated the isomeric distribution and rearrangement of complexes of the type $[CoXL_n]^{2+,3+}$ (where X = Cl^-, OH^-, H_2O, and L_n represents a pentadentate 13-, 14-, and 15-membered tetraaza or diaza–dithia (N_4 or N_2S_2) macrocycle bearing a pendant primary amine). The preparative procedures for chloro complexes produced almost exclusively kinetically preferred cis isomers (where the pendant primary amine is cis to the chloro ligand) that can be separated by careful cation-exchange chromatography. For L_{13} and L_{14} the so-called *cis-V* isomer is isolated as the kinetic product, and for L_{15} the *cis-VI* form (an N-based diastereomer) is the preferred, while for the L_{14}^S complex both *cis-V* and *trans-I* forms are obtained. All these complexes rearrange to form stable trans isomers in which the pendent primary amine is trans to the monodentate aqua or hydroxo ligand, depending on pH and the workup procedure. In total 11 different complexes have been studied. From these, two different trans isomers of $[CoClL_{14}^S]^{2+}$ have been characterized crystallographically for the first time in addition to a new structure of *cis-V*-$[CoClL_{14}^S]^{2+}$; all were isolated as their chloride perchlorate salts. Two additional isomers have been identified and characterized by NMR as reaction intermediates. The remaining seven forms correspond to the complexes already known, produced in preparative procedures. The kinetic, thermal, and baric activation parameters for all the isomerization reactions have been determined and involve large activation enthalpies and positive volumes of activation. Activation entropies indicate a very important degree of hydrogen bonding in the reactivity of the complexes, confirmed by density functional theory studies on the stability of the different isomeric forms. The isomerization processes are not simple and even some unstable intermediates have been detected and characterized as part of the above-mentioned 11 forms of the complexes. A common reaction mechanism for the isomerization reactions has been proposed for all the complexes derived from the observed kinetic and solution behavior.

Introduction

The use of tetradentate *N*-macrocyclic ligands coordinated to six-coordinate metal ions enables studies of ligand exchange reactions at the remaining two relatively labile coordination sites;[1−3] these studies are relevant to catalytic and electrochemical processes involving these compounds.[4−7] The chemistry of complexes derived from *cyclam* (1,4,8,-11-tetraazacyclotetradecane) and *cyclen* (1,4,7,10-tetraaza-

* To whom correspondence should be addressed. E-mail: manel.martinez@qi.ub.es.
[†] Departament de Química Inorgànica, Universitat de Barcelona.
[‡] Department of Chemistry, University of Queensland.
[§] Departament de Mineralogia, Cristal·lografia i Dipòsits Minerals, Universitat de Barcelona.

(1) Hung, Y.; Martin, L. Y.; Jackels, S. C.; Tait, A. M.; Busch, D. H. *J. Am. Chem. Soc.* **1977**, *99*, 4029−4039.
(2) Curtis, N.; Lawrance, G. A. *J. Chem. Soc., Dalton Trans.* **1985**, 1923−1927.
(3) Fallis, I. A. *Annu. Rep. Prog. Chem., Sect. A* **1999**, *95*, 313−351.
(4) Suzuki, T.; Hirai, Y.; Monjushiro, H.; Kaizaki, S. *Inorg. Chem.* **2004**, *43*, 6435−6444.
(5) Jones, D. R.; Lindoy, L. F.; Sargeson, A. M. *J. Am. Chem. Soc.* **1983**, *105*, 7327−7336.
(6) Humphry, T.; Forconi, M.; Williams, N. H.; Hengge, A. C. *J. Am. Chem. Soc.* **2004**, *126*, 11864−11869.
(7) Zibermann, I.; Maimon, E.; Cohen, H.; Meyerstein, D. *Chem. Rev.* **2005**, *105*, 2609−2625.

10.1021/ic060720s CCC: $33.50
Published on Web 09/14/2006

cyclododecane) ligands with different metal centers, particularly Co(III), has been throughly investigated,[3,8] and in some cases, the inclusion of substituents attached to the backbone nitrogen atoms have been introduced to tune reactivity.[9,10] Complexes of *cyclam* and its analogues can exist in two geometrical isomeric forms, that is, trans and cis, where the macrocycle is in a pseudo planar or folded configuration, respectively. The situation is far more complex than this though. Macrocyclic −NH− and −S− donors are chirotopic and may exist in one of two forms (*R*/*S*) which leads to the proliferation of diastereomeric forms.[11,12] Some interesting results concerning the involvement of donor-atom-based diastereomers in biologically relevant processes have appeared recently.[13,14] The use of pentadentate ligands that leave only a single coordination site capable of undergoing substitution processes is less common because of the more sophisticated nature of the ligands.[3,10,15,16] In most cases, a pentadentate ligand bearing predominantly strong field atoms is employed with a weakly bound monodentate ligand (e.g., chloro) completing the coordination sphere.[17−27]

We have been involved in the chemistry of cobalt(III) complexes with pentadentate macrocyclic ligands containing a pendant primary amine arm (Scheme 1).[28−31] The complexes have been prepared and characterized in pure isomeric

Scheme 1

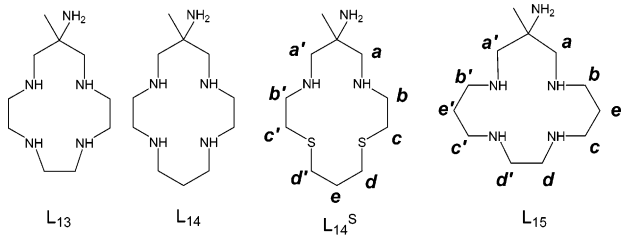

Scheme 2

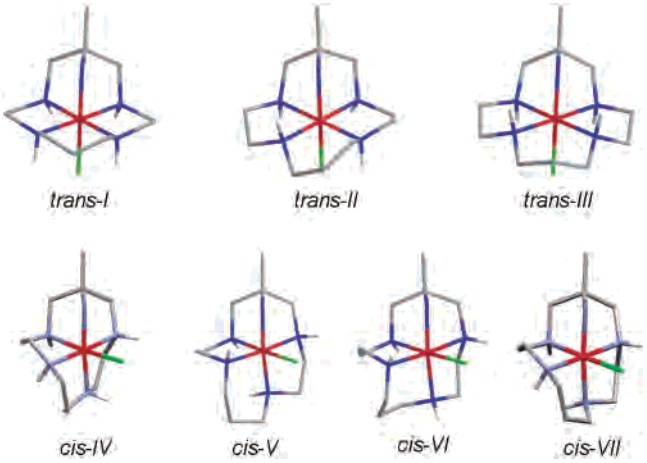

forms in a neutral or acidic medium, and their cis/trans isomerism has been established by X-ray crystallography.[28,30] In these cases the relative disposition of the primary amine and the monodentate sixth ligand define the cis or trans geometric isomer. The preferred isomeric form under these conditions is found to depend on the size of the ring, for example, the smaller the ring the greater preference for the cis isomeric form. Furthermore, even with the same cis/trans isomeric distribution, isomerism based on the configuration of the donor atoms is observed in some cases. The situation is rather similar to that observed for *cyclam* complexes, and the nomenclature for the isomeric forms observed in all cases, indicated for L_{14} in Scheme 2, is based on this similitude.[11] Note that for L_{14}^{S} lone pairs on the S donors provide a barrier to inversion as do the protons on a coordinated secondary amine.

The chemistry and stability of these complexes have been explored both by base hydrolysis studies of the corresponding chloro complexes, $[CoClL_n]^{2+}$,[28,32] and by outer-sphere redox processes between their aqua and phosphato derivatives with $[Fe^{II}(CN)_6]^{4-}$.[33,34] More recently, their use as building blocks for the preparation of Robin-Day *Class II* mixed-valence cyano-bridged Co(III)/Fe(II) complexes, that is, $[L_nCo^{III}(\mu\text{-}NC)Fe^{II}(CN)_5]^-$ and $[\{L_nCo^{III}(\mu\text{-}NC)\}_2Fe^{II}(CN)_4]^{2+}$, has been proved to be very successful.[35−37] Maintenance of the cis/trans isomeric form of the macrocycle is found to be possible on the mixed-valence complex provided carefully controlled

(8) Bernhardt, P. V.; Lawrance, G. A. *Comprehensive Coordination Chemistry*; Elsevier: Oxford, 2004; Chapter 6, pp 1−145.
(9) Bernhardt, P. V.; Hayes, E. J. *Inorg. Chem.* **2002**, *41*, 2892−2902.
(10) Bernhardt, P. V.; Lawrance, G. A. *Coord. Chem. Rev.* **1990**, *104*, 297−343.
(11) Bosnich, B.; Poon, C. K.; Tobe, M. L. *Inorg. Chem.* **1965**, *4*, 1102−1108.
(12) Adams, H.; Amado, A. M.; Félix, V.; Mann, B. E.; Antelo-Martinez, J.; Newell, M.; Ribeiro-Claro, P. J. A.; Spey, S. E.; Thomas, J. A. *Chem.—Eur. J.* **2005**, *11*, 2031−2046.
(13) Liang, X.; Parkinson, J. A.; Parsons, S.; Weishäulpl, M.; Sadler, P. J. *Inorg. Chem.* **2002**, *41*, 4539−4547.
(14) Liang, X.; Weishäulpl, M.; Parkinson, J. A.; Parsons, S.; McGregor, P. A.; Sadler, P. J. *Chem.—Eur. J.* **2003**, *9*, 4709−4717.
(15) Zhou, X.; Day, A. I.; Willis, A. C.; Jackson, W. G. *Chem. Commun.* **2003**, 2386−2387.
(16) Bonbieri, G.; Forsellini, E.; Del Pra, A.; Cooksey, C. J.; Humanes, M.; Tobe, M. L. *Inorg. Chim. Acta* **1982**, *61*, 43−49.
(17) Benzo, F.; Bernhardt, P. V.; González, G.; Martínez, M.; Sienra, B. *J. Chem. Soc., Dalton Trans.* **1999**, 3973−3979.
(18) Benzo, F.; González, G.; Martínez, M.; Sienra, B. *Inorg. React. Mech.* **2001**, *3*, 25−29.
(19) Curtis, N.; Lawrance, G. A. *Inorg. Chim. Acta* **1985**, *100*, 275−279.
(20) Curtis, N. J.; Lawrance, G. A.; Lay, P. A.; Sargeson, A. M. *Inorg. Chem.* **1986**, *25*, 484−488.
(21) Curtis, N. J.; Lawrance, G. A. *Inorg. Chem.* **1986**, *25*, 1033−1037.
(22) Curtis, N. J.; Lawrance, G. A.; van Eldik, R. *Inorg. Chem.* **1989**, *28*, 329−333.
(23) Dixon, N. E.; Lawrance, G. A.; Lay, P. A.; Sargeson, A. M. *Inorg. Chem.* **1983**, *22*, 846−847.
(24) Dixon, N. E.; Lancaster, M. J.; Lawrance, G. A.; Sargeson, A. M. *Inorg. Chem.* **1981**, *20*, 470−476.
(25) Lawrance, G. A.; Schneider, K.; van Eldik, R. *Inorg. Chem.* **1984**, *23*, 3922−3925.
(26) González, G.; Martínez, M.; Rodríguez, E. *J. Chem. Soc., Dalton Trans.* **1995**, 891−892.
(27) González, G.; Martínez, M.; Rodríguez, E. *Eur. J. Inorg. Chem.* **2000**, 1333−1338.
(28) Hambley, T. W.; Lawrance, G. A.; Martínez, M.; Skelton, B. W.; White, A. L. *J. Chem. Soc., Dalton Trans.* **1992**, 1643−1648.
(29) Lawrance, G. A.; Martínez, M.; Skelton, B. W.; White, A. H. *Aust. J. Chem.* **1991**, *44*, 113−121.
(30) Lawrance, G. A.; Manning, T. M.; Maeder, M.; Martínez, M.; O'Leary, M. A.; Patalinghug, W.; Skelton, A. W.; White, A. G. *J. Chem. Soc., Dalton Trans.* **1992**, 1635−1641.
(31) Lawrance, G. A.; Martínez, M.; Skelton, B. W.; White, A. G. *J. Chem. Soc., Dalton Trans.* **1992**, 1649−1652.
(32) Baran, Y.; Lawrance, G. A.; Martínez, M.; Wilkes, E. *Inorg. React. Mech.* **2000**, *1*, 315−318.
(33) Martínez, M.; Pitarque, M. A. *J. Chem. Soc., Dalton Trans.* **1995**, 4107−4111.
(34) Martínez, M.; Pitarque, M.; van Eldik, R. *Inorg. Chim. Acta* **1997**, *256*, 51−59.

reaction conditions are maintained.[38] Under less controlled conditions isomerization of the complexes from their mononuclear geometric forms to other geometries is often observed. This isomerization is commonly associated with the workup in an alkaline medium, while at acidic pH values these reactions take place only on a time scale of months at room temperature.[17,36] In the literature there are good examples of the changes observed in some of the preparative processes for the complex $[CoClL_{15}]^{2+}$, including crystallographic characterizations.[17,30,39] In view of the important differences in the stability and reactivity of these various isomeric forms and their use as building blocks for mixed-valence complexes, where the importance of diasteroisomerism has been recently indicated,[40] we present in this paper the study of their isomeric distribution at acidic and alkaline pH values. We have also carried out a density functional theory (DFT) analysis on the corresponding chloro, aqua, and hydroxo complexes of these isomeric forms to examine the influence of strain within the macrocyclic ring in addition to effects due to the monodentate ligand and the polarity of the medium.

Experimental Section

Safety note: *Although we have experienced no problems with the compounds in this work, perchlorate salts are potentially explosive and should only be handled in small quantities, never scraped from sintered glass frits, and never heated while in the solid state.*

Syntheses. The complex cations *cis-V*-$[CoClL_{13}]^{2+}$, *cis-V*-$[CoClL_{14}]^{2+}$, *trans-I*-$[CoClL_{14}]^{2+}$, *cis-VI*-$[CoClL_{15}]^{2+}$, *trans-II*-$[CoClL_{15}]^{2+}$, and *cis-V*-$[CoClL_{14}{}^{S}]^{2+}$ have been prepared as described previously in the literature.[17,28,30,35,41] All the complexes have been characterized by their ^{1}H NMR, ^{13}C NMR, and UV−vis spectra. Table S1 (Supporting Information) collects all the relevant data.

Complexes *trans-I*-$[CoClL_{14}{}^{S}]Cl(ClO_4)$ and *trans-III*-$[CoClL_{14}{}^{S}]Cl(ClO_4)$ were prepared by reaction at pH 7 between $CoCl_2$ and $L_{14}{}^{S}\cdot 3HCl$ in equimolecular amounts (35×10^{-3} mol), as described for the *cis-V*-$[CoClL_{14}{}^{S}]^{2+}$ complex. The final reaction mixture was diluted to 5000 cm^3 and charged on a Dowex 50W × 2, and a red {2+}-charged band (1 M HCl) was eluted. This band comprised a mixture of isomeric forms that was taken to dryness by evaporation at room temperature and reduced pressure. A more rigorous chromatrographic separation was conducted on a longer Dowex 50W × 2 column. The *cis-V*-$[CoClL_{14}{}^{S}]^{2+}$ isomer eluted first and was isolated in a 10% yield by evaporation of the eluent to a small volume and addition of $HClO_4$ to afford the mixed chloride perchlorate salt. The second band produced, after concentration of the eluate to about 15 cm^3 and addition of a few drops of concentrated $HClO_4$, a solid in a 20% yield, which was characterized as *trans-III*-$[CoClL_{14}{}^{S}]Cl(ClO_4)$ by elemental analysis [calcd (found): H, 5.1 (5.4); C, 26.8 (26.9); N, 8.5 (8.5)], UV−vis and ^{13}C NMR spectroscopy (Table S1, Supporting Information), and X-ray crystallography. A third more diffuse band of the same charge produced, after concentration of the eluate at room temperature to approximately 5 cm^3 and addition of a few drops of concentrated $HClO_4$, a solid in a 5% yield. It was characterized as *trans-I*-$[CoClL_{14}{}^{S}]Cl(ClO_4)$ by elemental analysis [calcd (found): H, 5.1 (5.7); C, 26.8 (26.8); N, 8.5 (8.6)], UV−vis and ^{13}C NMR spectroscopy (Table S1, Supporting Information), and X-ray crystallography.

The two recovered *cis-V*-$[CoClL_{14}{}^{S}]^{2+}$ compounds were obtained from the above-mentioned first band of the preparative procedure, *cis-V*-$[CoClL_{14}{}^{S}]Cl(ClO_4)$ crystallized from a solution of dilute HCl and $HClO_4$ and *cis-V* $[CoClL_{14}{}^{S}]Cl_2\cdot 3H_2O$ isolated from the HCl solution alone.

Physical Methods. NMR spectra were recorded on a Varian Mercury-400 (^{1}H, 400 MHz or ^{13}C 100.6 MHz) instrument in D_2O/H_2O (8/2 to 2/8) and using NaTSP as external standard at the Serveis Científico-Tècnics de la Universitat de Barcelona. Elemental analyses were carried out also by the Serveis Científico-Tècnics de la Universitat de Barcelona. UV−vis spectra were recorded on HP5482A, Cary50, or J&M TIDAS instruments depending on the circumstances, as indicated below.

Crystallography. For compounds *cis-V*-$[CoClL_{14}{}^{S}]Cl(ClO_4)$ and *trans-I*-$[CoClL_{14}{}^{S}]Cl(ClO_4)$ cell constants at 293 K were determined by a least-squares fit to the setting parameters of 25 independent reflections measured on an Enraf-Nonius CAD4 four-circle diffractometer employing graphite-monochromated Mo Kα radiation (0.710 73 Å) and operating in the $\omega-2\theta$ scan mode within the range $3 < 2\theta < 50°$ for *cis-V*-$[CoClL_{14}{}^{S}]Cl(ClO_4)$ and $4.8 < 2\theta < 64°$ for *trans-I*-$[CoClL_{14}{}^{S}]Cl(ClO_4)$. For the structure of *trans-III*-$[CoClL_{14}{}^{S}]Cl(ClO_4)$ a MAR345 diffractometer with image plate detection was employed. Data reduction and empirical absorption corrections (Ψ scans) were performed (for *cis-V*-$[CoClL_{14}{}^{S}]Cl(ClO_4)$) with the WINGX suite of programs.[42] Structures were solved by direct methods using the SHELXS computer program[43] and refined by the full-matrix least-squares method with the SHELX97 computer program.[44] All non-H atoms were refined with anisotropic thermal parameters except minor contributors to disorder. All H atoms were included at estimated positions using a riding model. Molecular structure diagrams (Figure 1) were produced with ORTEP3.[45] Crystal and refinement data are summarized in Table 1, and selected bond lengths and angles are summarized in the caption of Figure 1.

Kinetics. Reactions were followed by UV−vis spectroscopy in the full 800−300 nm range. Observed rate constants were derived from the absorbance versus time traces at wavelengths where a maximum increase and/or decrease of absorbance was observed. No dependence of the observed rate constant values on the selected wavelengths was detected, as expected for reactions where a good retention of isosbestic points is observed. The general kinetic technique is that previously described,[46,47] in all cases pseudo-first-

(35) Bernhardt, P. V.; Macpherson, B. P.; Martínez, M. *Inorg. Chem.* **2000**, *39*, 5203−5208.
(36) Bernhardt, P. V.; Bozoglián, F.; González, G.; Martínez, M.; Macpherson, B. P.; Sienra, B. *Inorg. Chem.* **2006**, *45*, 74−82.
(37) Bernhardt, P. V.; Bozoglián, F.; Macpherson, B. P.; Martínez, M. *Coord. Chem. Rev.* **2005**, *249*, 1902−1916.
(38) Bernhardt, P. V.; Macpherson, B. P.; Martínez, M. *J. Chem. Soc., Dalton Trans.* **2002**, 1435−1441.
(39) Bernhardt, P. V.; Martínez, M. *Inorg. Chem.* **1999**, *38*, 424−425.
(40) D'Alessandro, D. M.; Dinolfo, P. H.; Davies, M. S.; Hupp, J. T.; Keene, F. R. *Inorg. Chem.* **2006**, *45*, 3261−3274.
(41) Wei, G.; Allen, C. C.; Hambley, T.; Lawrance, G. A.; Maeder, M. *Inorg. Chim. Acta* **1997**, *261*, 197−200.
(42) Farrugia, L. J. *J. Appl. Crystallogr.* **1999**, *32*, 837−838.
(43) Sheldrick, G. M. *SHELXS*; Univeristät of Göttingen: Göttingen, Germany, 1997.
(44) Sheldrick, G. M. *SHELX97, Programs for Crystal Structure Analysis*, release 97-2; Universität Göttingen: Göttingen, Germany, 1998.
(45) Farrugia, L. J. *J. Appl. Crystallogr.* **1997**, *30*, 565.
(46) Bernhardt, P. V.; Bozoglián, F.; Macpherson, B. P.; Martínez, M.; González, G.; Sienra, B. *Eur. J. Inorg. Chem.* **2003**, 2512−2518.
(47) Bernhardt, P. V.; Bozoglián, F.; Macpherson, B. P.; Martínez, M.; Merbach, A. E.; González, G.; Sienra, B. *Inorg. Chem.* **2004**, *43*, 7187−7195.

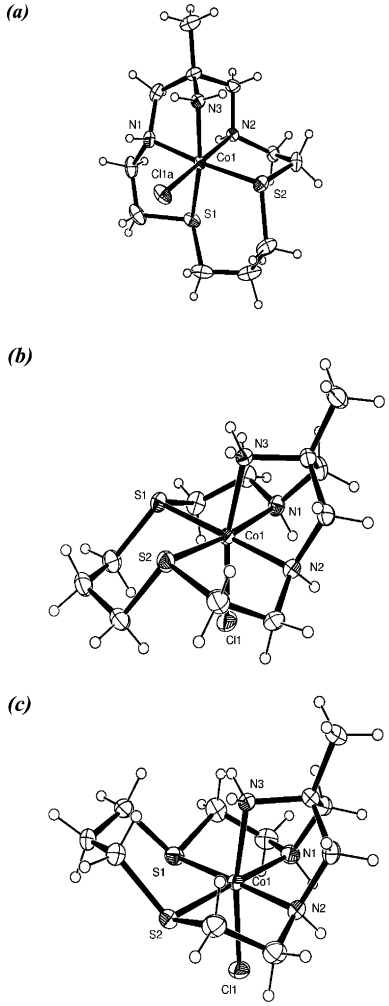

Figure 1. (a) Drawing of cation 1 within the structure of *cis-V*-[$CoClL_{14}^{S}$]-$Cl(ClO_4)$ (30% ellipsoids shown). Coordinate bond lengths (Å) and angles (deg): cation 1, Co1−N1 1.951(4), Co1−N3 1.956(3), Co1−N2 1.966(3), Co1−S1 2.214(1), Co1−S2 2.222(1), Co1−Cl1A 2.244(1), N1−Co1−N3 79.7(2), N1−Co1−N2 91.2(2), N3−Co1−N2 85.7(1), N1−Co1−S1 86.7-(1), N3−Co1−S1 165.3(1), N2−Co1−S1 89.0(1), N1−Co1−S2 174.5(1), N3−Co1−S2 94.8(1), N2−Co1−S2 88.7(1), S1−Co1−S2 98.84(5), N1−Co1−Cl1A 91.4(1), N3−Co1−Cl1A 91.2(1), N2−Co1−Cl1A 175.5(1), S1−Co1−Cl1A 94.77(5), S2−Co1−Cl1A 88.36(5); cation 2, Co2−N3B 1.953(3), Co2−N2B 1.960(3), Co2−N1B 1.969(3), Co2−S2B 2.216(1), Co2−S1B 2.228(1), Co2−Cl1B 2.241(1), N3B−Co2−N2B 81.1(2), N3B−Co2−N1B 85.3(1), N2B−Co2−N1B 90.4(1), N3B−Co2−S2B 167.8(1), N2B−Co2−S2B 87.9(1), N1B−Co2−S2B 89.7(1), N3B−Co2−S1B 96.4-(1), N2B−Co2−S1B 177.4(1), N1B−Co2S1B 88.8(1), S2B−Co2−S1B 94.59(5), N3B−Co2−Cl1B 89.8(1), N2B−Co2−Cl1B 90.2(1), N1B−Co2−Cl1B 174.9(1), S2B−Co2−Cl1B 95.42(5), S1B−Co2−Cl1B 90.35(5). (b) Drawing of the cation within the structure of *trans-III*-[$CoClL_{14}^{S}$]$Cl(ClO_4)$ (30% ellipsoids shown). Coordinate bond lengths (Å) and angles (deg): Co1−N2 1.964(1), Co1−N3 1.950(1), Co1−N1 1.977(1), Co1−S2 2.2218-(7), Co1−S1 2.2174(9), Co1−Cl1 2.2611(7), N2−Co1−N3 85.84(5), N2−Co1−N1 91.14(6), N3−Co1−N1 81.41(5), N2−Co1−S2 89.73(4), N3−Co1−S2 91.17(4), N1−Co1−S2 172.44(4), N2−Co1−S1 178.76(4), N3−Co1−S1 93.99(4), N1−Co1−S1 90.05(4), S2−Co1−S1 89.04(2), N2−Co1−Cl1 87.23(5), N3−Co1−Cl1 168.11(3), N1−Co1−Cl1 89.09(5), S2−Co1−Cl1 98.46(3), S1−Co1−Cl1 93.14(3). (c) Drawing of the cation within the structure of *trans-I*-[$CoClL_{14}^{S}$]$Cl(ClO_4)$ (30% ellipsoids shown). Coordinate bond lengths (Å) and angles (deg): Co1−N2 1.978(3), Co1−N3 1.949(2), Co1−N1 1.978(3), Co1−S2 2.212(1), Co1−S1 2.199(1), Co1−Cl1 2.264(1), N2−Co1−N3 83.9(1), N2−Co1−N1 90.5(1), N3−Co1−N1 83.7(1), N2−Co1−S2 89.43(8), N3−Co1−S2 97.68(9), N1−Co1−S2 178.57(9), N2−Co1−S1 178.75(9), N3−Co1−S1 97.38(8), N1−Co1−S1 89.37(9), S2−Co1−S1 90.68(4), N2−Co1−Cl1 89.58(9), N3−Co1−Cl1 170.13(8), N1−Co1−Cl1 88.99(9), S2−Co1−Cl1 89.58(5), S1−Co1−Cl1 89.17(5).

order conditions were maintained ([OH^-] or [H^+] >10 × [Co]; ionic strength was kept at 1.0 M with $LiClO_4$. The cobalt complex concentration was kept in the (3−5) × 10^{-3} M margin, and rate constants were independent of the concentration of the metal species. At atmospheric pressure, runs were recorded on a Cary50 or HP8452A instrument, equipped with a thermostated multicell transport. For runs at elevated pressure, a previously described pressurizing system and high-pressure cell were used.[48,49] In these cases the absorbance versus time traces were recorded on a Cary[50] instrument at a fixed wavelength chosen from the atmospheric pressure experiments. Alternatively a J&M TIDAS instrument was also used in the full wavelength range. All the values obtained for the pseudo-first-order rate constants as a function of the metal complex, temperature, pressure and [OH^-] or [H^+] are collected in Table S2 (Supporting Information).

DFT Calculations. Calculations were carried out with the GAUSSIAN98 package,[50] and the hybrid density function method known as B3LYP was applied.[51,52] Effective core potentials (ECP) were used to represent the innermost electrons of the cobalt atoms and the basis set of valence double-ς quality associated with the pseudopotentials known as LANL2DZ.[53] A similar description was used for heavy elements such as chlorine or sulfur,[54] supplemented with an extra *d*-polarization function.[55] The basis set for the light elements such as O, N, C, and H was 6-31G*.[56,57] Energies in aqueous solutions were taken into account by polarizable continuum model (PCM) calculations (water, ϵ = 78.39),[58,59] keeping the geometry optimized for gas phase (single-point calculations).

Results

Synthesis and Structural Characterization. The preparation of the various complexes in this work as isomerically stable (non-interconverting) mixtures has been achieved with the standard procedures described in the literature;[28−31,38] in all cases extensive slow chromatography workup at [HCl] = 1.5−2.0 M on Dowex 50W × 2 columns is needed for the separation of equally {2+}-charged chloro complexes.

(48) Crespo, M.; Font-Bardía, M.; Granell, J.; Martínez, M.; Solans, X. *Dalton Trans.* **2003**, 3763−3769.
(49) Favier, I.; Gómez, M.; Granell, J.; Martínez, M.; Font-Bardía, M.; Solans, X. *Dalton Trans.* **2004**, 123−132.
(50) Frisch, M. J.; Trucks, G. W.; Schlegel, H. B.; Scuseria, G. E.; Robb, M. A.; Cheeseman, J. R.; Zakrzewski, V. G.; Montgomery, J. A.; Stratmann, R. E.; Burant, J. C. Dapprich, S.; Millam, J. M.; Daniels, A. D.; Kudin, K. N.; Strain, M. C.; Farkas, O.; Tomasi, J.; Barone, V.; Cossi, M.; Cammi, R.; Mennucci, B.; Pomelli, C.; Adamo, C.; Clifford, S.; Ochterski, J.; Petersson, G. A.; Ayala, P. Y.; Cui, Q.; Morokuma, K.; Salvador, P.; Dannenberg, J. J.; Malick, D. R.; Rabuck, A. D.; Raghavachari, K.; Foresman, J. B.; Ciolowski, J.; Ortiz, J. V.; Baboul, A. G.; Stefanov, B. B.; Liu, G.; Liashenko, A.; Piskorz, P.; Komaromi, I.; Gomperts, R.; Martin, R. L.; Fox, D. J.; Keith, T.; Al-Laham, M. A.; Peng, C.; Nanayakkara, A.; Challacombe, M.; Gill, P. M. W.; Johnson, B.; Chen, W.; Wong, M. W.; Andres, J. L.; Gonzalez, C.; Head-Gordon, M.; Replogle, E. S.; Pople, J. A. *Gaussian 03*, revision C.02; Gaussian Inc.: Wallingford, CT, 2004.
(51) Becke, A. D. *J. Chem. Phys.* **1993**, *98*, 5648−5652.
(52) Lee, C.; Yang, W.; Parr, R. G. *Phys. Rev. B* **1988**, *37*, 785−789.
(53) Hay, P. J.; Wadt, W. R. *J. Chem. Phys.* **1985**, *82*, 299−310.
(54) Hay, P. J.; Wadt, W. R. *J. Chem. Phys.* **1985**, *82*, 270−273.
(55) Höllwarth, A.; Böhme, M.; Dapprich, S.; Ehlers, A. W.; Gobbi, A.; Jonas, V.; Köhler, K. F.; Stegman, R.; Veldkamp, A.; Frenking, G. *Chem. Phys. Lett.* **1993**, *208*, 237−240.
(56) Hariharan, P. C.; Pople, J. A. *Theor. Chim. Acta* **1973**, *28*, 213−222.
(57) Francl, M. M.; Petro, W. J.; Hehre, W. J.; Binkley, J. S.; Gordon, M. S.; DeFrees, D. J.; Pople, J. A. *J. Chem. Phys.* **1982**, *77*, 3654−3665.
(58) Tomasi, J.; Persico, M. *Chem. Rev.* **1994**, *94*, 2027−2094.
(59) Amovilla, C.; Barone, V.; Cammi, R.; Cancès, E.; Cossi, M.; Mennucci, B.; Pomelli, C. S.; Tomasi, J. *Adv. Quantum Chem.* **1998**, *32*, 227−261.

Table 1. Crystal Data for Complexes *cis-V*-[$CoClL_{14}^{S}$]$Cl(ClO_4)$, *trans-I*-[$CoClL_{14}^{S}$]$Cl(ClO_4)$, and *trans-III*-[$CoClL_{14}^{S}$]$Cl(ClO_4)$

	cis-V-[$CoClL_{14}^{S}$]$Cl(ClO_4)$	*trans-I*-[$CoClL_{14}^{S}$]$Cl(ClO_4)$	*trans-III*-[$CoClL_{14}^{S}$]$Cl(ClO_4)$
formula	$C_{11}H_{25}Cl_3CoN_3O_4S_2$	$C_{11}H_{25}Cl_3CoN_3O_4S_2$	$C_{11}H_{25}Cl_3CoN_3O_4S_2$
fw	492.74	492.74	492.74
crystal system	monoclinic	orthorhombic	monoclinic
space group	$P2_1/a$ (No. 14, variant)	*Pbca* (No. 61)	$P2_1/c$ (No. 14)
a, Å	14.004(1)	12.908(3)	8.790(4)
b, Å	17.321(2)	12.997(3)	15.412(6)
c, Å	17.171(2)	22.96(2)	14.423(5)
β, deg	113.948(8)		104.57(2)
V	3806.5(7)	3851(3)	1891(1)
Z	8	8	4
D_c	1.720	1.700	1.731
R_1 (obs. data)	0.0363	0.0313	0.0313
wR_2 (all data)	0.0934	0.0692	0.0821

For the $[CoClL_{13}]^{2+}$ system, the *cis-V* isomer is obtained as a single product, as expected.[30] However, for the $[CoClL_{14}]^{2+}$, $[CoClL_{15}]^{2+}$, and $[CoClL_{14}^{S}]^{2+}$ systems the number of isolated isomeric forms present in the reaction mixture is greater than than that found when the original preparative methods were followed.[28−30,41] The careful control of the pH and workup procedures represents the key difference in the new methodology used.

For the $[CoClL_{14}]^{2+}$ system, complex *cis-V*-$[CoClL_{14}]^{2+}$ is obtained as the first fraction eluting when the reaction medium is kept at pH < 6;[30] following this fraction, small quantities of isomer *trans-I*-$[CoClL_{14}]^{2+}$ are also obtained. When the reaction is carried out at pH > 8, *trans-I*-$[CoClL_{14}]^{2+}$ becomes the major product[38] and only small quantities of *cis-V*-$[CoClL_{14}]^{2+}$ are obtained. No *trans-III*-$[CoClL_{14}]^{2+}$ is obtained in either of the procedures.[28] Although *trans-III*-$[CoClL_{14}]^{2+}$ has been reported and characterized crystallographically, it is only obtained by a slow isomerization reaction upon long standing for a period of months in acidic conditions; a similar situation has been reported for $[CoL_{15}(OH_2)]^{3+}$ systems.[18]

The situation for the $[CoClL_{15}]^{2+}$ system follows the same pattern. Although the initial preparative methods produced almost exclusively the *cis-VI*-$[CoClL_{15}]^{2+}$ complex,[30] its *trans-II* form was later identified using a different synthesis[17] which produces a mixture of both isomers that can be separated chromatographically. The *cis-VI* isomer elutes first from the column, well ahead of the *trans-II* isomer. Characterization of both bands is accomplished by spectroscopic comparison with literature data.[17,30] The relative amounts resulting from the preparative procedure of the two isomeric forms is found to be, as for the L_{14} system, extremely dependent on the pH of the reaction medium and the time used for the workup. That is, short reaction times and/or pH values lower than 6 produced almost exclusively the *cis-VI* form of the complex, while long workup times at pH > 8 produced exclusively the *trans-II* isomer. It is interesting that the isomeric *trans-III* form has been characterized in aqua and mixed-valence complexes[17,39] even though this form is not detected during the preparation of the chloro complexes.

The preparation of the $[CoClL_{14}^{S}]^{2+}$ complex produces a far more complicated isomeric mixture. The *cis-V* isomer has been characterized previously, and crystal structures of $[Co(OAc)L_{14}^{S}](ClO_4)_2\cdot H_2O$[29] and $[CoClL_{14}^{S}](ClO_4)_2\cdot H_2O$[41] have been reported. Here we report an additional crystal structure of *cis-V*-$[CoClL_{14}^{S}]^{2+}$, namely, *cis-V*-$[CoClL_{14}^{S}]Cl(ClO_4)$, crystallized from a solution of dilute HCl and $HClO_4$. Two crystallographically independent cations were present, but both in the same conformation (Figure 1a) and exhibiting the same coordination environment (see caption to Figure 1a). One of the perchlorate anions was disordered (about a common Cl-atom site), and two sets of O atoms were resolved and refined with complementary occupancies (70:30). The coordinate bond lengths and angles are very similar to those found in $[CoClL_{14}^{S}](ClO_4)_2\cdot 2H_2O$.[41]

Although the cis isomers are the only ones crystallized from a simple Co(III)/L_{14}^{S} complexation reaction,[29,41] the *trans-III* form is obtained in the mixed valence $[L_{14}^{S}Co^{III}(\mu\text{-NC})Fe^{II}(CN)_5]^-$ species,[60] and this configuration is retained in the one-electron oxidized $[L_{14}^{S}Co^{III}(\mu\text{-NC})Fe^{III}(CN)_5]$.[47] The preparative procedure for the chloro complex reveals, during Dowex 50W × 2 column chromatography, three well-separated bands. The first corresponds to *cis-V*-$[CoClL_{14}^{S}]^{2+}$, as assigned on the basis of its known UV−vis and ^{13}C MNR spectra.[30] The second band shows a ^{13}C NMR spectrum with a set of seven signals, which indicates that the complex has a symmetry plane consistent with either the *trans-I* or the *trans-III* form (Scheme 2). The X-ray crystal structure of the complex isolated as its perchlorate salt is shown in Figure 1b where the *trans-III* isomeric form is apparent. The six-membered chelate ring containing both S-donors adopts a chair conformation, and the two macrocyclic five-membered chelate rings adopt a staggered conformation. No special features are evident in the structure, and the coordinate bond lengths and angles are very similar to those found in the structures of $[L_{14}^{S}Co^{III}(\mu\text{-NC})Fe^{II}(CN)_5]^-$ and $[L_{14}^{S}Co^{III}(\mu\text{-NC})Fe^{III}(CN)_5]$,[40,47] as well as the mononuclear *cis-V* isomer (Figure 1a).

Importantly, the ^{13}C NMR resonances of *trans-III*-$[CoClL_{14}^{S}]^{2+}$ are essentially the same as those observed in the spectrum of $[L_{14}^{S}Co^{III}(\mu\text{-NC})Fe^{II}(CN)_5]^-$.[40] Indeed the ^{13}C NMR resonances of the coordinated L_{14}^{S} ligand have

(60) Bernhardt, P. V.; Bozoglián, F.; Macpherson, B. P.; Martínez, M. *Dalton Trans.* **2004**, 2582−2587.

been found to be independent of the nature of the sixth ligand on the $\{CoL_n\}^{3+}$ core (Supporting Information, Table S1),[35] and this is useful in assigning this *trans-III* isomeric form when crystallographic evidence is absent.

The third band from the column is isolated in the same manner yielding a ^{13}C NMR spectrum bearing seven signals distinct from the ones associated to the *trans-III* isomer. A mirror plane of symmetry is again present, so by elimination this complex must be assigned to the *trans-I*-$[CoClL_{14}^{S}]^{2+}$ form. This was confirmed by crystallography (Figure 1c). An interesting feature is that the N3−Co1−S1 and N3−Co1−S2 coordinate angles are widened by more than 4° in the *trans-I* isomer than the *trans-III* isomer. The origin of this difference appears to be nonbonded H···H repulsion between the primary amine and the methylene groups adjacent to the S-donors on the six-membered chair chelate ring. Also of note is that the two macrocyclic five-membered rings are now in an eclipsed conformation.

Solution Behavior. In view of the distribution of the isomeric forms of the complexes indicated above,[35−38,60] we proceeded to the study of their relative stability in solution. All the systems were studied as chloro complexes in 0.1 M HCl (to suppress base hydrolysis of the chloro complex), as hydroxo complexes in 0.1 M NaOH (which form after the few seconds in alkaline solution)[28,32] and as aqua complexes, obtained after acidification of the hydroxo complexes with 6 M $HClO_4$. In all cases, the signal of the methyl group in the ^1H NMR spectra proved to be the best spectroscopic signal for this purpose. Even so, high fields (400 MHz) had to be used to obtain significant results with good resolution. The position of the methyl signal is also well clear of the intense signal from H_2O, introduced during base and acid hydrolysis of the chloro precursors. Scheme 3 summarizes all the isomerization processes observed that are described in the next paragraphs.

For the *cis-V*-$[CoClL_{13}]^{2+}$ complex, the solutions obtained dissolving a crystalline sample in 0.1 M HCl revealed a single signal in the ^1H NMR spectrum at 1.39 ppm that did not change with time. Dissolution of the complex in 0.1 M NaOH produced a solution with a single, time-independent resonance at 1.33 ppm, while the aqua complex yielded a single peak at 1.43 ppm.

The same chemistry on the $[CoClL_{14}]^{2+}$ complexes was more complicated and time dependent. The macrocyclic methyl signals in the ^1H NMR spectrum of the chloro and aqua cobalt(III) complexes, in their *trans-I* and *cis-V* forms, remain unchanged over a period of days at room temperature. The *trans-I*-$[Co(OH)L_{14}]^{2+}$ complex shows a methyl signal that remains constant for days in 0.1 M NaOH (1.28 ppm). The *cis-V*-$[Co(OH)L_{14}]^{2+}$ complex signal at 1.33 ppm is replaced by the peak of the *trans-I* isomer within a period of days (Figure S1a). In all cases, protonation of the OH^- ligand by $HClO_4$ produced the expected aqua complexes with the same isomerism.

For complexes with the L_{15} macrocycle the behavior is quite similar; in this case even the elusive *trans-III* form of the $\{CoL_{15}\}^{3+}$ moiety can be detected in solution.[17] While the crystallographically characterized *cis-VI* and *trans-II* forms of $[CoClL_{15}]^{2+}$ are stable for long periods in 0.1 M HCl, their hydroxo derivatives rearrange over time. A solution of *trans-II*-$[CoClL_{15}]^{2+}$ in 0.1 M NaOH produced immediately, even at 0 °C, a ^1H NMR spectrum with two signals at 1.38 and 1.33 ppm in an 8:1 ratio. The system does not evolve further with time, and ^{13}C NMR (requiring longer acquisition times) could be used for characterization of the species; the more intense set of resonances gave 12 ^{13}C NMR peaks, while the minor form gave 7. The set of more intense signals is exactly the same as that for the asymmetric *trans-II*-$\{CoL_{15}\}$, while the less intense agrees with that for a *trans-III* form as found in $[L_{15}Co^{III}(\mu\text{-NC})\text{-}Fe^{II}(CN)_5]^-$. Acidification of the alkaline solution with 6 M $HClO_4$ produces two new signals in the ^1H MNR spectrum in the same 8:1 ratio (1.36 and 1.35 ppm, respectively) assigned to the *trans-II* and *trans-III* aqua complexes by ^{13}C NMR spectroscopy.

When *cis-VI*-$[CoClL_{15}]^{2+}$ is dissolved in 0.1 M NaOH, the signal at 1.38 ppm corresponding to the *cis-VI*-$[Co(OH)\text{-}L_{15}]^{2+}$ disappears over a period of 1 h at room temperature. The signal is replaced by the identical resonances in the same 8:1 mixture of *trans-II* and *trans-III* hydroxo complexes; no other signals are observed in the final reaction mixture (Figure S1b, Supporting Information).

For the $\{CoL_{14}^{S}\}^{3+}$ system, the dynamic behavior is much more complex, as expected from the results obtained in the preparative procedures. Even though the chloro complexes in the *cis-V* and *trans-III* forms do not change for days at room temperature when dissolved in 1.0 M HCl, *trans-I*-$[CoClL_{14}^{S}]^{2+}$ rearranges very slowly and neatly to the *trans-III* form, as monitored by ^1H NMR (Figure S1c). Surprisingly, no isomerization of the *trans-I*-$[CoL_{14}^{S}(OH_2)]^{3+}$ is observed. In 0.1 M NaOH all three of the isolated isomeric forms of the hydroxo complexes produced the changes indicated below.

For the *cis-V* form (Figure 2) initial appearance a signal at 1.21 ppm corresponding to the *trans-III* hydroxo form occurs a short time after dissolution. Another signal of the same intensity at 1.36 ppm appears after a while, and thereafter these two signals (1.21 and 1.36 ppm) maintain the same ratio (ca. 1:1) until their complete disappearance in favor of a new signal at 1.46 ppm. The same sequence is obtained when the study is carried out with the *trans-III* isomeric form as a precursor, but in this case the initial signal at 1.21 ppm (*trans-III*) decreases in favor of that at 1.36 ppm (*cis-V*); no signal is detected initially at 1.46 ppm. The equilibrium established between the *cis-V* and the *trans-III* forms evolves slowly to a single final complex. The sequence of NMR spectral changes indicates that the slow process initiates on the *cis-V* form. The structure of the final species is not obvious: its methyl proton resonance does not correspond to any of the complexes characterized. The ^{13}C NMR spectrum of the solution has a set of 11 signals (23.8, 36.0, 36.8, 36.9, 43.6, 43.7, 53.1, 57.4, 60.5, 63.5, 64.5 ppm), which indicates asymmetry of the complex. Either a cis (different from *cis-V*) or a *trans-II* arrangement of the macrocycle (Scheme 2) of the $\{CoL_{14}^{S}\}$ core would be consistent with this spectrum. The *trans-II* form of the

Scheme 3

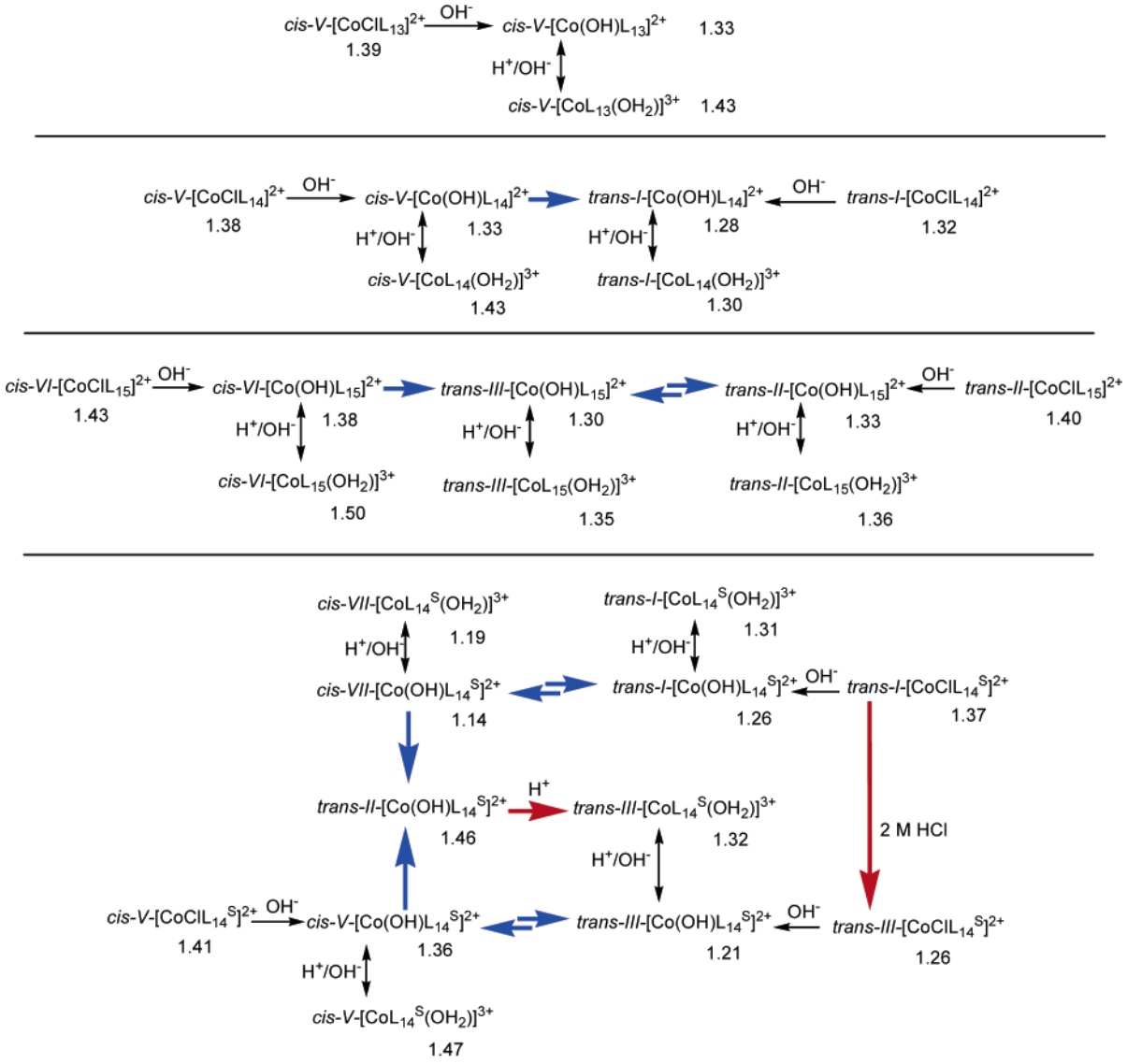

Source of OH^-: aqueous 0.2 M NaOH
Source of H^+: aqueous 6 M $HClO_4$, unless stated
δ values in ppm in H_2O/D_2O mixtures
Colored bold arrows indicate the isomerization steps observed

macrocycle is more likely, as the proximity of the two sets of signals at 36.8/36.9 and 43.6/43.7 ppm indicates a similar magnetic environment of carbons **a**/**a′** and **b**/**b′** (Scheme 1) according to the stereochemistry indicated in Scheme 2. Addition of 6 M $HClO_4$ to the putative *trans-II*-$[Co(OH)L_{14}{}^S]^{2+}$ produces, during the time scale needed for the NMR experiment, the *trans-III*-$[CoL_{14}{}^S(OH_2)]^{3+}$ complex, assigned from the 1.32 ppm signal of the pendant methyl group. The first formed *trans-II*-$[CoL_{14}{}^S(OH_2)]^{3+}$ is not observed.

Similarly, when the *trans-I*-$[CoClL_{14}{}^S]^{2+}$ complex is dissolved in 0.1 M NaOH the initial hydroxo signal (1.26 ppm) evolves to a new signal at 1.14 ppm that does not correspond to any of the known species (Supporting Information, Table S1). On further standing, both signals disappear in favor of that corresponding to the above-mentioned putative *trans-II* form until it becomes the only one in the spectrum. As before, acidification of the mixture produces solely the *trans-III*-$[CoL_{14}{}^S(OH_2)]^{3+}$ complex with $\delta(CH_3)$ = 1.32 ppm. The ^{13}C NMR analysis of the solution, containing the above-mentioned new isomeric form with a $\delta(CH_3)$ signal at 1.14 ppm, shows a set of 11 signals at 23.8, 28.6, 30.4, 33.7, 37.4, 38.9, 48.1, 53.3, 55.7, 58.5, and 58.7 ppm. These were assigned to a *cis-VII* isomeric form of the complex, on the basis of the sequence of changes observed during isomerization, when compared with those observed for the *trans-III*/*cis-V*/*trans-II* derivatives (see Discussion). Again, no *trans-II* form of the macrocycle is observed until some buildup of the *cis-VII* form becomes significant, indicating that the process producing the *trans-II* arrangement originates from this putative *cis-VII* isomer.

DFT Stability Studies. We have carried out DFT calculations to determine the relative stability in water of each of

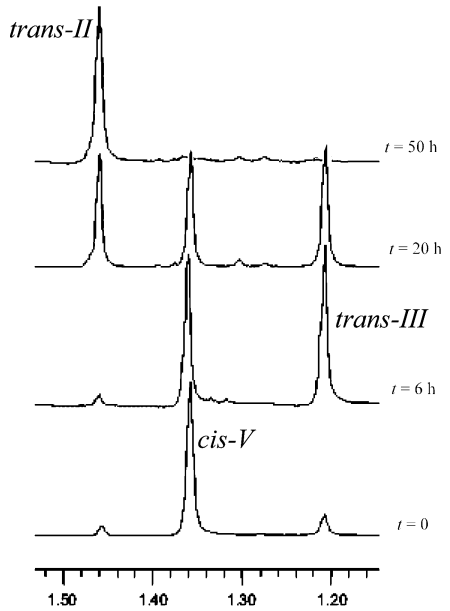

Figure 2. Variation with time of the methyl zone of the 400 MHz ^{1}H NMR spectra of a 0.1 M NaOH solution of 5×10^{-2} M *cis-V*-[Co(OH)-$L_{14}{}^S$]$^{2+}$ (50 °C, H_2O/D_2O, NaTMSP reference).

the isomers involved, depending on L_n and X in $[CoXL_n]^{2+;3+}$ (X = Cl^-, OH^-, and H_2O; L_n = L_{14}, L_{15}, and $L_{14}{}^S$). Relative energies in a water solution are shown in Figure 3. They have been estimated using the continuum dielectric model approximation on the optimized energy of the complexes in the gas phase (Supporting Information).

The optimized molecular geometries for the $\{CoL_{14}\}$ system are very similar in all cases; only small differences can be found between the different isomers. The Co−X distances are 2.25 (Cl), 1.85 (OH), and 2.06 (OH_2) Å, while the Co−N(H) and Co−N(H_2) distances are within the 1.94−2.02 and 1.95−2.06 Å range, the shortest being for the *cis-V* form and the longest for the *trans-III* form. Calculations predict *trans-I*-$[CoXL_{14}]^{2+;3+}$ as the most stable isomer for all complexes. The appearance of this form after long isomerization reaction times is then expected on thermodynamic grounds, in good agreement with the experimental results. The *cis-V*-$[CoClL_{14}]^{2+}$ to *trans-I* evolution is consistent with a calculated stabilization energy of 20 kJ mol^{-1} (Figure 3a).

Taking into account the similar predicted stability of the *trans-I* and *trans-III* isomers for X = Cl^- or H_2O (<1 kJ mol^{-1}), the formation of equilibrium mixtures of the two isomeric forms of these complexes is expected. Nevertheless, under the conditions used in this study, only isomer *trans-I* has been observed. Transformation from *trans-I* to *trans-III* must take place via the *trans-II* form through consecutive inversions of coordinated amines (see Discussion), and the thermodynamic instability of the intermediate makes this pathway unfavorable.

A survey of cobalt(III) complexes having a similar skeleton to those in this work within the *Cambridge Structural Database* (Supporting Information, Table S3) confirms the higher stability of *trans-I* (thermodynamic) and *cis-V* (kinetic) isomers.[30,35,38,60−63] Besides the above-mentioned *trans-III*-$[CoClL_{14}]^{2+}$ formed over a period of months from the *cis-V* isomer (an atypical synthesis), the *trans-II* configuration has been seen in the chloro complex of a diamino-substituted macrocyclic analogue of L_{14}. This compound shows a very strong hydrogen bond between the protonated (uncoordinated) primary amonium group and a water of crystallization ($RNH_3{}^+\cdots OH_2$ distance 1.92 Å).[64]

The optimized molecular geometries for the L_{15} system are also very similar for each isomer (Supporting Information). Despite the lack of clear trends, Co−X distances are always longer for the cis than for the trans isomeric forms. Figure 3b shows the relative stability of L_{15} complexes when a continuum dielectric has been introduced as solvent, representing an important disagreement with the experimental results, and no *trans-III* forms are expected. We suspect that the influence of a different degree of hydrogen bonding must play a key role in the relative energies. Intramolecular NH···Cl contact distances of less than 2.5 Å are found for all isomers, except for *trans-III* with distances longer than 2.68 Å. Some of the reactivity mechanistic parameters determined (see Discussion) agree with this fact.

The molecular geometries of $L_{14}{}^S$ are equivalent to the related L_{14} pentaamine complexes; Co−X and Co−N distances have similar values, differences being less than 0.01 Å in most of the complexes. The Co−S bond distances are in the narrow 2.28−2.32 Å range, while the rest of the parameters do not show any clear trend. Energy calculations for chloro and hydroxo complexes indicate that the *trans-III* forms are the most stable, followed by *cis-V*, while the *trans-I* and *trans-II* forms are even higher in energy (Figure 3c). For the aqua complexes all the isomeric forms have similar energies (within a 10 kJ mol^{-1} margin), indicating that all the forms should be observed in solution after isomerization. Crystallographically, all $[CoXL_{14}]^{m+}$ complexes correspond to *trans-I* (X = Cl^-, Figure 1c), *trans-III* (X = Cl^-; Figure 1b, $\{Fe^{II}(CN)_6\}^{4-}$, $\{Fe^{III}(CN)_6\}^{3-}$),[47,60] or *cis-V* (X = Cl^- (Figure 1a), AcO^-)[29,41] forms.

Kinetics. Given the dynamic behavior of some of the systems studied, we pursued the study of any further information that could be derived from the kinetic and activation parameters for the isomerization processes. The simplest process studied corresponds to that from *trans-I*-$[CoClL_{14}{}^S]^{2+}$ to *trans-III*-$[CoClL_{14}{}^S]^{2+}$, occurring at low pH. The process is found to be clean and independent of proton or complex concentrations at $[H^+] > 1 \times 10^{-2}$ M, and the value obtained for k_{obs} (Supporting Information, Table S2) corresponds to the simple first-order isomerization reaction, k_{iso}. At pH > 2 hydrolysis of the chloro complex competes with isomerization, and a mixture of reactions is observed, obscuring the observation of the simpler *trans-I*-$[CoClL_{14}{}^S]^{2+}$

(61) Bernhardt, P. V.; Macpherson, B. P. *Acta Crystallogr., Sect. C* **2003**, m467−m470.
(62) Bernhardt, P. V.; Macpherson, B. P. *Acta Crystallogr., Sect. C* **2003**, m533−m536.
(63) Macpherson, B. P.; Alzoubi, B. M.; Bernhardt, P. V.; Martínez, M.; Tregloan, P.; van Eldik, R. *Dalton Trans.* **2005**, 1459−1467.
(64) Curtis, N. F.; Robinson, W. T.; Weatherburn, D. *Aust. J. Chem.* **1992**, *45*, 1663−1680.

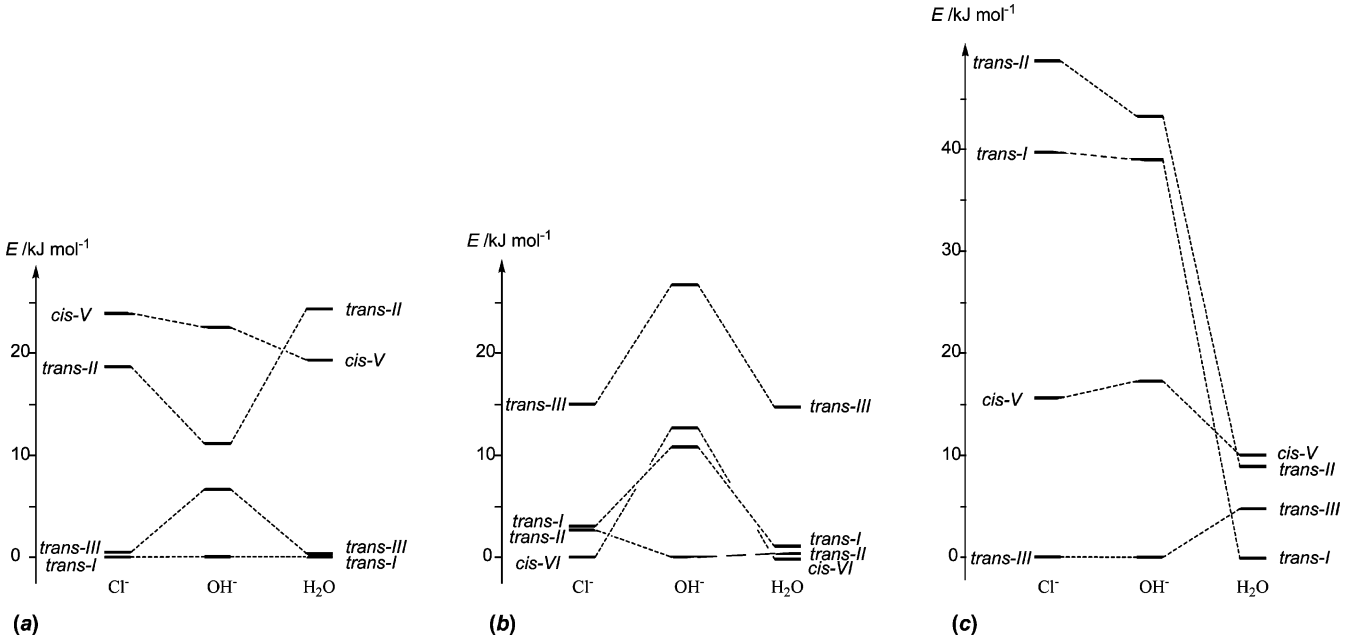

Figure 3. Calculated relative stability for each isomer for complexes of type $[CoX(L_n)]^{m+}$ (X = Cl^-, OH^-, and OH_2) in water: (a) L_{14}; (b) L_{15}; (c) L_{14}^S. Only the observed forms are represented for clarification (complete table of values is available in Supporting Information).

Table 2. Values of the Kinetic, Thermal, and Baric Activation Parameters Determined for the Isomerization Systems Studied (I = 1.0 M $LiClO_4$)

L_n	process	$^{298}k_{iso}$, s^{-1}	$\Delta H^{\ddagger}$, kJ mol^{-1}	$\Delta S^{\ddagger}$, J K^{-1} mol^{-1}	$\Delta V^{\ddagger}$ (T), cm^3 mol^{-1} (K)
L_{14}	*cis-V* → *trans-I*[a]	6.0×10^{-6}	120 ± 1	60 ± 2	21 ± 1 (332)
L_{15}	*cis-VI* → {*trans-II* ⇌ *trans-III*}[a]	1.3×10^{-3}	127 ± 9	120 ± 30	16 ± 1 (288)
L_{14}^S	*cis-V* ⇌ *trans-III*[a]	5.0×10^{-4}	100 ± 1	30 ± 2	13 ± 1 (328)
	cis-V → *trans-II*[a]	5.0×10^{-6}	101 ± 5	−6 ± 18	19 ± 1 (293)
	trans-I ⇌ *cis-VII*[a]	4.0×10^{-4}	93 ± 6	−12 ± 17	16 ± 2 (316)
	cis-VII → *trans-II*[a]	5.0×10^{-6}	98 ± 9	−18 ± 26	16 ± 1 (343)
	trans-I → *trans-III*[b]	1.5×10^{-6}	108 ± 2	3 ± 4	∼0

[a] Hydroxo complexes in 0.1 M NaOH. [b] Chloro complexes in 0.1 M HCl.

to *trans-III*-$[CoClL_{14}^S]^{2+}$ process. Figure S2 (Supporting Information) illustrates the changes in the UV−vis spectrum for the process. The monitoring of the process at variable temperature and pressure produced the corresponding kinetic and activation parameters for the process that are collected in Table 2. The value determined for ΔH^+ is quite large while the values found for $\Delta S^{\ddagger}$ and $\Delta V^{\ddagger}$ are close to zero, indicating that an important degree of organization/compression should be present in the transition state of the reaction.

The reactions occurring at alkaline pH have to be related to base-assisted processes, for which the well-established conjugate-base mechanism applies.[65,66] The rate law that can be derived for these reactions is indicated in eq 1, which shows how k_{obs} approaches the first-order rate constant k_{iso} asymptotically at high $[OH^-]$ and/or K_{dep} values.

$$k_{obs} = \frac{k_{iso}K_{dep}[OH^-]}{1 + K_{dep}[OH^-]} \qquad (1)$$

UV−vis monitoring of alkaline solutions of the complexes that undergo isomerization produced well behaved absorbance versus time first-order traces. Retention of isosbestic points is also observed, as expected from the neat reactions monitored by NMR. Figure 4 collects some of these variations, and Table S2 (Supporting Information) collects all the pseudo-first-order observed rate constants for the reactions studied as a function of the process, $[OH^-]$, temperature, and pressure. The general trend of these values is in excellent agreement with equation 1 (Figure S3, Supporting Information), producing a limiting value of k_{iso} at $[OH^-] > 0.01$ M in all cases. The temperature and pressure dependence of k_{iso} was consequently determined from the values of k_{obs} at $[OH^-] = 0.1$ M. Table 2 collects the kinetic and activation parameters for all the systems studied; the values were derived from the standard Eyring and ln k versus P plots (Figure 5).

The values obtained for $\Delta H^{\ddagger}$ are in all cases in good agreement with the expected high enthalpic demand of a dissociative activation. The values of the volumes of activation are positive. Finally, the set of values for $\Delta S^{\ddagger}$ are surprising. Only for the L_{15} complexes are the values positive enough to be in agreement with the highly dissociative activation process associated with the large values of $\Delta H^{\ddagger}$. While for the L_{14} ligand complex the value is still positive, although less than the expected for a dissociatively activated process, for the L_{14}^S complexes the values determined are near to zero in all cases. Again the different nature of

(65) Tobe, M. L.; Burgess, J. *Inorganic Reaction Mechanisms*; Longman: Harlow, U.K., 1999.
(66) Wilkins, R. G. *Kinetics and Mechanisms of Reactions of Transition Metal Complexes*; VCH: Weinheim, 1991.

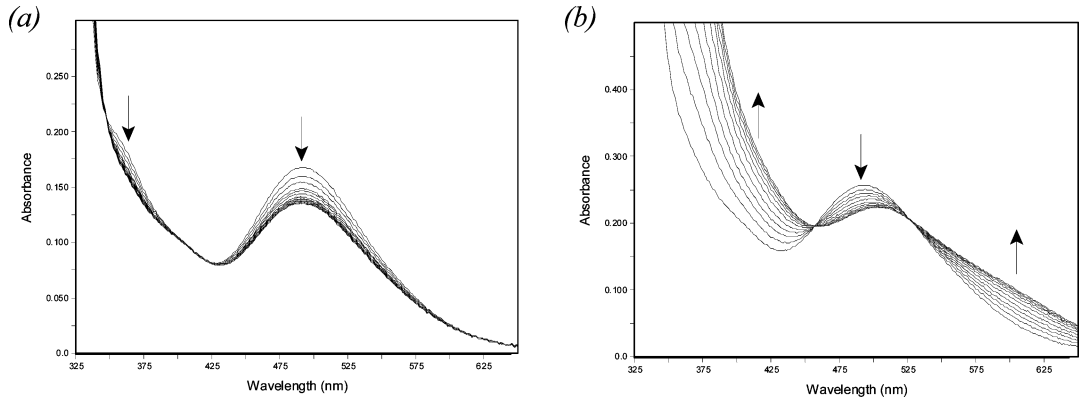

Figure 4. UV−vis monitoring of the isomerization processes studied at $[OH^-] = 0.1$ M on *cis-V*-$[Co(OH)L_{14}^S]^{2+}$ ($[Co] = 1 \times 10^{-3}$ M, $I = 1.0$ ($LiClO_4$)). (a) *cis-V* ⇌ *trans-III* process at 20 °C, 3 h; (b) {*cis-V* ⇌ *trans-III*} → *trans-II* process at 50 °C and 300 atm, 6 h.

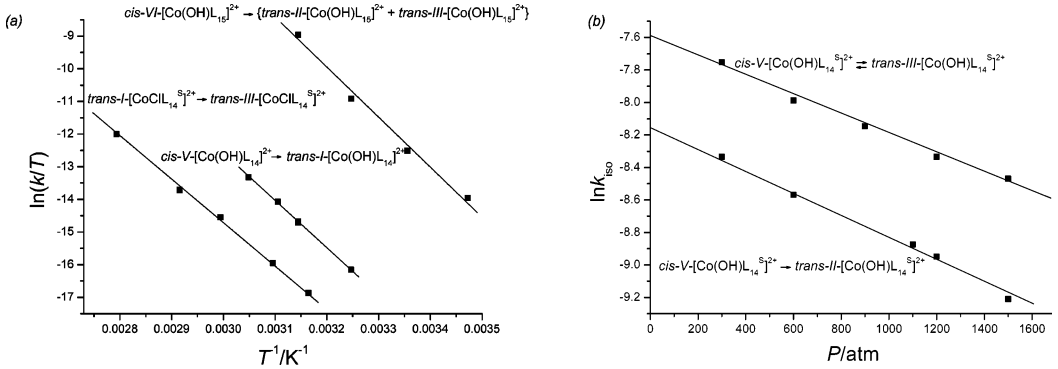

Figure 5. (a) Eyring plots for the isomerization reactions *cis-V*-$[Co(OH)L_{14}]^{2+}$ → *trans-I*-$[Co(OH)L_{14}]^{2+}$, *cis-VI*-$[Co(OH)L_{15}]^{2+}$ → {*trans-II*-$[Co(OH)L_{15}]^{2+}$ + *trans-III*-$[Co(OH)L_{15}]^{2+}$}, and *trans-I*-$[CoClL_{14}^S]^{2+}$ → *trans-III*-$[CoClL_{14}^S]^{2+}$. (b) ln *k* vs *P* plots for the isomerization reactions *cis-V*-$[Co(OH)L_{14}^S]^{2+}$ ⇌ *trans-III*-$[Co(OH)L_{14}^S]^{2+}$ (293 K) and *cis-V*-$[Co(OH)L_{14}^S]^{2+}$ → *trans-II*-$[Co(OH)L_{14}^S]^{2+}$ (328 K).

pentaamine and triaminedithiaether systems have to be responsible for this fact.

Discussion

Observations on the Preparative Procedure. All the isomerization processes observed agree, in general, with the thermodynamic preference for a more symmetrical trans arrangement of the macrocycle. Only the *cis-V*-$\{CoL_{13}\}^{3+}$ core does not undergo any isomerization reaction, given the exceptionally small size of the macrocyclic ligand.[1,67] For the larger macrocycles, all the complexes obtained kinetically from preparative procedures are found in cis geometries. It seems clear that, with the exception of the L_{14}^S ligand, a kinetically preferred cis folded conformation of the coordinated macrocycle is formed that rearranges subsequently to a trans geometry just like for *cyclam* complexes.[68,69] The processes only take place under catalyzed conditions, given the extreme inertness of the Co(III) center,[28,32−34] and the nature of the final trans form depends on the systems at hand. Scheme 3 summarizes the processes observed. Complete *trans-III* forms of the L_{14} and L_{15} ligands are only obtained by prolonged standing.[28,39] Hydrogen bonding can be held responsible for this fact; an amine proton interacts with the OH^- ligand in the *trans-II* form, producing some stabilization. The change of the ligand for a less electronegative group causes loss of this extra stability and the *trans-III* form becomes the most stable. DFT calculations agree with the importance of intramolecular hydrogen bonding in the stabilization of the different forms of the L_{15} complexes. While in the gas phase the *cis-VI*, *trans-I*, *trans-II*, and *trans-III* complexes fall within a narrow energy margin of 4 kJ mol^{-1} (Table S4b, Supporting Information), the results become those indicated in Figure 3 when a dielectric continuum is applied. The discrepancy with the experimental results can only be associated with the involvement of structurized water molecules in the solvent, as indicated by lack of parallelism between $\Delta S^{\ddagger}$ and $\Delta V^{\ddagger}$ in the processes studied.

The pattern for the L_{14}^S macrocycle system is even more complex. The longer Co−S bonds in the $\{CoL_{14}^S\}^{3+}$ core, and the presence of two nonbonding electron pairs in the thiaether donor atoms produce important differences. Labilization of the systems by base induces a transformation of the two *cis-V* and *trans-I* isomeric forms of the complexes to a final putative *trans-II* form, stable as the hydroxo complex, which rearranges instantly to the final stable *trans-III* aqua derivative upon addition of acid. The highly strained[11] *cis-VII* hydroxo complex is detected as a postulated intermediate in the {*trans-I* ⇌ *cis-VII*} → *trans-II* → *trans-III* sequence. Probably the existence of intramolecular hydrogen bonding interactions is responsible of the existence of this highly strained isomeric form.

(67) Curtis, N. J.; Hendry, P.; Lawrance, G. A. *J. Chem. Soc., Dalton Trans.* **1988**, 47−51.
(68) Hay, R. W.; You-Quan, C. *Inorg. Chim. Acta* **1991**, *180*, 147−149.
(69) Hambley, T. *J. Chem. Soc., Dalton Trans.* **1986**, 565−569.

Scheme 4

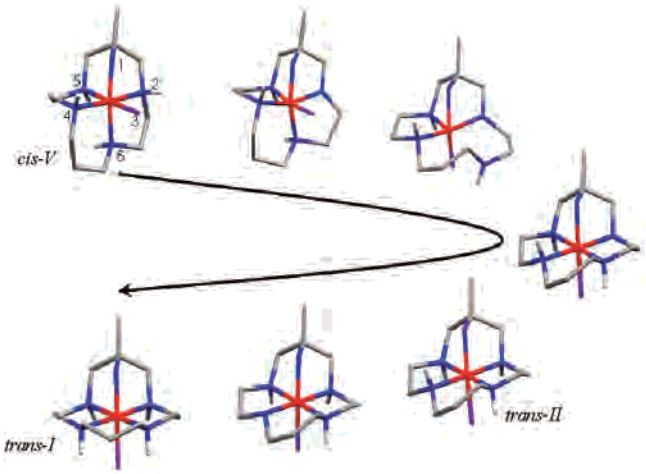

Isomerization Mechanisms. Although the simplest base-catalyzed isomerization process observed, *cis-V*-$[Co(OH)L_{14}]^{2+}$ to *trans-I*-$[Co(OH)L_{14}]^{2+}$, occurs without the presence of any intermediate complex, it involves the inversion or migration of more than one donor atom. The deprotonation/dissocation/rearrangement/protonation of the amines 2, 4, and 6 sequence indicated in Scheme 4 produces the final *trans-I*-$\{CoL_{14}\}^{3+}$ core.

The planarity of deprotonated amines is a key step both for dissociative activation and nitrogen inversion.[70] This type of sequence has already been held responsible for similar processes on Ni(II) *cyclam* derivatives.[71−73] The very high calculated energy of the intermediate *trans-II* form is probably responsible for its non-detection. The sequence shown in Scheme 4 can also be applied to the L_{15} hydroxo complexes. The instant equilibrium between the *trans-II* and *trans-III* forms of $[Co(OH)L_{15}]^{2+}$ is explained by a simple acid−base process,[70] and the *cis-VI* to *trans-III* process follows the same steps as mentioned above. The consequence is that the enthalpy of activation of the isomerization processes for both L_{14} and L_{15} complexes should practically be the same and correspond to the dissociation of a Co−NH (macrocycle) bond, as observed in Table 2. The difference in $\Delta S^{\ddagger}$ can be related to the smaller size of the L_{14} ligand not allowing a larger disorganization of the system upon dissociation. The important increase in volume should be related both to dissociation and to involvement of the free RR′NH group in hydrogen bonding with the solvent.

For the base-assisted isomerization of $[Co(OH)L_{14}{}^{S}]^{2+}$ the process can be visualized in a similar way. The lack of NH groups in positions 3 or 4 makes the arrangement between trans complexes in alkaline medium less straightforward than a simple acid−base equilibrium.[70] A proper base-catalyzed dissociation of a Co−S bond (acid−base equilibrium of amine 2 or 5, plus dissociation/inversion of three or four thiaethers) is needed. The process is inherently different to the thioether inversion observed for other inert cobalt systems,[74] where the nonmacrocyclic nature of the ligand allowed for a simple inversion with no dissociation, as found for other systems.[75] The values found for $\Delta H^{\ddagger}$ collected in Table 2 agree with this fact. For all the base-assisted processes the values are the same within error and approximately 25−30 kJ mol^{-1} lower than for the pentaamine L_{14} and L_{15} systems, in good correlation with the different strengths of the Co−amine and Co−thiaether bonds.[76] The volumes of activation are positive, as expected for a dissociatively activated mechanism, and slightly lower than for the pentaammine systems, given the already longer Co−S bonds.[28,29] As for $\Delta S^{\ddagger}$, the values are extremely low (practically zero) for the dissociative activation of the mechanism proposed, even for a 14-membered macrocyle which is well-matched to the size of the Co(III) ion (see above).[27,34] Dissociation of a thiaether group during the activation process produces the appearance of two nonbonding electron pairs capable of organizing the solvation sphere of the complex. This effect, doubling de facto that indicated above for the pentaamine complexes, has to be the responsible for the values obtained.

The processes observed for the acid-catalyzed isomerization of $[CoXL_{14}{}^{S}]^{2+}$ ($X = OH^{-}$, Cl^{-}) systems merit a separate discussion. The fast *trans-II*-$[Co(OH)L_{14}{}^{S}]^{2+}$ to *trans-III*-$[CoL_{14}{}^{S}(OH_2)]^{3+}$ reaction has to be related to inversion of the thiaether group in position 3. The process is, de facto, parallel to that observed for the *trans-II*/*trans-III* equilibrium of the $[Co(OH)L_{15}]^{2+}$ complex. The more complex and slow *trans-I*-$[CoClL_{14}{}^{S}]^{2+}$ to *trans-III*-$[CoClL_{14}{}^{S}]^{2+}$ process involves the inversion of both thiaether groups. The probability of a double movement is very low, and the process has to first generate a *trans-II*-$[CoClL_{14}{}^{S}]^{2+}$ complex, which rapidly produces the final *trans-III*-$[CoClL_{14}{}^{S}]^{2+}$ complex (Figure 3c). As a consequence the values of the activation parameters shown in Table 2 should relate to the inversion of one thiaether group in positions 3 or 4. The values for the thermal activation parameters, $\Delta H^{\ddagger}$ and $\Delta S^{\ddagger}$, are of the same magnitude as those measured for the base assisted reaction, while the volume of activation is zero. Although a simple acid-assisted dissociation of the thiaether group would explain the values obtained, the $[H^{+}]$-independent values of k_{iso} at pH = 2 do not agree with the expected high acidity of the coordinated thioether ligands. Inversion of the thioether via planar coordination, similar to that of amides, to the metal center agrees much better with the results observed.[74,75,77] The process goes via a compressed/organized transition state with less hydrogen-bonded water molecules, which compensates the expected decrease in entropy and volume.

(70) Clarkson, A. J.; Buckingham, D. A.; Blackman, A. G.; Clark, C. R. *Inorg. Chem.* **2000**, *39*, 4769−4775.
(71) Lee, D.; Suh, M. P.; Lee, J. W. *J. Chem. Soc., Dalton Trans.* **1997**, 577−584.
(72) Lincoln, S. F.; Coates, J. A.; Hadi, D. A.; Pisaniello, D. L. *Inorg. Chim. Acta* **1984**, *81*, L9−L10.
(73) Maimon, E.; Zilbermann, I.; Cohen, H.; Kost, D.; van Eldik, R.; Meyerstein, D. *Eur. J. Inorg. Chem.* **2005**, 4997−5005.
(74) Jackson, W. G.; Sargeson, A. M. *Inorg. Chem.* **1978**, *17*, 2165−2169.
(75) Font-Bardía, M.; Gallego, C.; González, G.; Martínez, M.; Merbach, A. E.; Solans, X. *Dalton Trans.* **2003**, 1106−1113.
(76) Huheey, J. E.; Keiter, L. A.; Keiter, R. L. *Inorganic Chemistry: Principles of Structure and Reactivity*; Harper and Collins: New York, 1993.
(77) van Diemen, J. H.; Haasnoot, J. G.; Hage, R.; Reedijk, J.; Vos, J. G.; Wang, R. *Inorg. Chem.* **1991**, *30*, 4038.

Conclusions

The extensive study of the formation of the series of $[CoClL_n]^{2+}$ complexes, from cobalt(II) salts and the ligand, indicates a general kinetic preference for the folded, cis, conformation of the macrocycles in the compounds. Labilization of the systems produced the final thermodynamically more stable pseudo-planar, trans, forms. This labilization occurs through base-assisted dissociatively activated processes of the macrocylic ligand for all the systems. However, when thiaether donors are present in the ligand, L_{14}^S, spontaneous reactions leading to the inversion of the S-donors of the macrocycle are also observed.

The mechanism for the isomerization processes has been studied at variable acidities, temperature, and pressure for all the systems. The results indicate a common donor atom movement sequence leading to the thermodynamically stable isomer; in total 11 forms have been detected in solution. DFT calculations of the relative energies of 15 different forms studied do not agree with the relative stability observed after thermodynamic equilibration of the systems. The existence of intramolecular hydrogen bonding interactions dominates some of the calculated structures, indicating that not only a dielectric continuum has to be taken into account. The same type of bonding interactions with the aqueous solvent should be considered. In this respect the activation parameters determined for the isomerization processes are an excellent proof of such solvent involvement.

Acknowledgment. Financial support for this work was provided by DGI, Grants CTQ2006-14909-C02-02/BQU and CTQ2005-08123-C02-02/BQU, and by DURSI, Grant 2005SGR-0036. Computing resources at the CESCA were made available in part through a grant of *Fundació Catalana per a la Recerca*. P.V.B. wishes to thank the Australian Research Council for financial support, and B.P.M. acknowledges the award of a University of Queensland Graduate School Travel Award that enabled his visit to Barcelona.

Supporting Information Available: Crystallographic data in CIF format; optimized calculated structures for the complexes studied in PDB format; values of k_{obs} determined as a function of the complex, $[OH^-]$, temperature, and pressure; ^1H (CH_3), ^{13}C, and UV−vis spectra characterization data for all the complex species prepared in this work; relative energies for the different $[CoXL_n]^{3;2+}$ complexes; and structures found in CSD of the isomers considered in this paper. Also plots of the variation with time of the ^1H NMR spectra of *cis-V*-$[Co(OH)L_{14}]^{2+}$, *cis-VI*-$[Co(OH)L_{15}]^{2+}$, and *trans-I*-$[CoClL_{15}]^{2+}$ and of the UV−vis spectra of the *trans-I*-$[CoClL_{14}^S]^{2+}$. A plot of k_{obs} vs $[OH^-]$ for the reaction *cis-VI*-$[Co(OH)L_{15}]^{2+} \rightarrow$ {*trans-II*-$[Co(OH)L_{15}]^{2+}$ + *trans-III*-$[Co(OH)L_{15}]^{2+}$} at 25 °C, I = 1.0 ($LiClO_4$), is also included. This material is available free of charge via the Internet at http://pubs.acs.org.

IC060720S